



1 **Holocene glaciation in the Rwenzori Mountains, Uganda**

2 Margaret S. Jackson^{1*}, Meredith A. Kelly¹, James M. Russell², Alice M. Doughty³, Jennifer A.

3 Howley^{1^}, Susan R.H. Zimmerman⁴, Bob Nakileza⁵

4

5 1. Earth Sciences, Dartmouth College, Hanover, NH, United States

6 2. Earth, Environmental, and Planetary Sciences, Brown University, Providence, RI United

7 States

8 3. Geology, Bates College, Lewiston, ME

9 4. Center for Accelerator Mass Spectrometry, Lawrence Livermore National Laboratory,

10 Livermore, CA United States

11 5. Mountain Resource Centre, Makerere University, Kampala, Uganda

12 *Current address: School of Geography, Archaeology, and Irish Studies, National University of

13 Ireland Galway, Galway, Ireland

14 ^Current address: New Hampshire Department of Health and Human Services, Concord, NH,

15 United States

16 Correspondence to: Margaret S. Jackson (margaret.jackson@nuigalway.ie)

17

18

19

20

21

22

23



24 **Abstract**

25 Tropical glaciers are retreating rapidly, threatening alpine ecosystems across the low latitudes.
26 Understanding how tropical glaciers responded to past periods of warming is crucial for
27 predicting and adapting to future climate change, yet relatively little is known about glacial
28 fluctuations in tropical regions during the recent past (i.e., the Holocene Epoch). This is
29 particularly true in the African tropics, where data constraining the timing and magnitude of
30 Holocene glacial fluctuations in the region are sparse and where temperatures during the Middle
31 Holocene were perhaps as warm as or warmer than today. Here we present new beryllium-10
32 surface-exposure ages that constrain Holocene glacial extents in the equatorial Rwenzori
33 Mountains, Uganda. These results document rapid Early Holocene (~11.7-8.2 ka) glacial retreat
34 in two separate catchments and indicate that Late Holocene (~4.2 ka-present) deposits mark the
35 greatest expansion of Rwenzori glaciers during the last ~11 ka. Holocene glacial fluctuations
36 elsewhere in tropical Africa and in tropical South America are broadly similar to those in the
37 Rwenzori, with most tropical glaciers retreating rapidly during the Early Holocene and
38 remaining near or inboard of their Late Holocene positions through much of Holocene time. The
39 similarity of Holocene glacial fluctuations across the tropics implies that low-latitude glaciers
40 responded to a common forcing mechanism, most likely temperature. Although the drivers of
41 Holocene temperature changes in the tropics remain enigmatic, these data help constrain the
42 expression of tropical temperature changes in the low latitudes.

43

44

45

46



47 **1 Introduction**

48 The ongoing, coherent retreat of Earth's alpine glaciers is unique within the Holocene
49 Epoch (~11.7 ka-present; Walker et al., 2012) and emblematic of anthropogenic warming
50 (Solomina et al., 2015). The loss of alpine glaciers is of particular concern in the tropics, where
51 high-elevation regions are warming at a rate twice the global average (Vuille et al., 2008).
52 Tropical glaciers are a primary source of freshwater and are a fundamental component of
53 regional economies, underpinning agriculture, hydropower, and tourism (Bradley et al., 2006;
54 Chevallier et al., 2011). Accurately projecting the response of glaciers to future climate change is
55 thus crucial for effective community response and adaptation (Stocker et al., 2013), and these
56 projections rely on robust understanding of the sensitivity of tropical glaciers to past climate
57 conditions.

58 Tropical glaciers respond to changes in both temperature and precipitation, although the
59 relative influence of these forcings depends upon a glacier's unique climatic setting (Sagredo et
60 al., 2014). Recent work to reconstruct past glacial fluctuations in tropical South America
61 indicates that glaciers there were near or inboard of their Late Holocene (~4.2 ka-present; Walker
62 et al., 2012) maxima during much of the Holocene Epoch (Jomelli et al., 2014; Solomina et al.,
63 2015; Stansell et al., 2017). Although relatively little is known about Holocene glacial
64 fluctuations in the African tropics (Kaser and Osmaston, 2002; Solomina et al., 2015), recently
65 produced terrestrial paleotemperature reconstructions provide greater paleoclimatic context for
66 understanding past changes in tropical African glacial extent (Weijers et al., 2007; Tierney et al.,
67 2008; Woltering et al., 2011; Loomis et al., 2012, 2017). Of particular interest is the response of
68 glaciers to climate conditions during the Middle (~8.2-4.2 ka) and Early (~11.7-8.2 ka) Holocene
69 Epoch (Walker et al., 2012), when temperatures in tropical Africa may have been similar to or



70 higher than modern (Ivory et al., 2017 and references therein). Determining when and how
71 glaciers in the African tropics fluctuated during past warm periods provides crucial information
72 for assessing whether, or how long, tropical glaciers may persist under future warming scenarios.
73 Here we present new data from the equatorial Rwenzori Mountains of Uganda (0.3°N,
74 30.0°E; Figure 1) that constrain the extent of glaciers in two separate valleys during the
75 Holocene. These data include twelve beryllium-10 (^{10}Be) surface-exposure ages of glacial
76 landforms which provide evidence of past glacial extents in the Rwenzori during Holocene time.
77 We then compare the Rwenzori glacial chronology with records of East African glaciation and
78 paleoclimate to assess both the potential drivers of past glacial fluctuations as well as the
79 response of these glaciers to changes in Holocene climate.
80

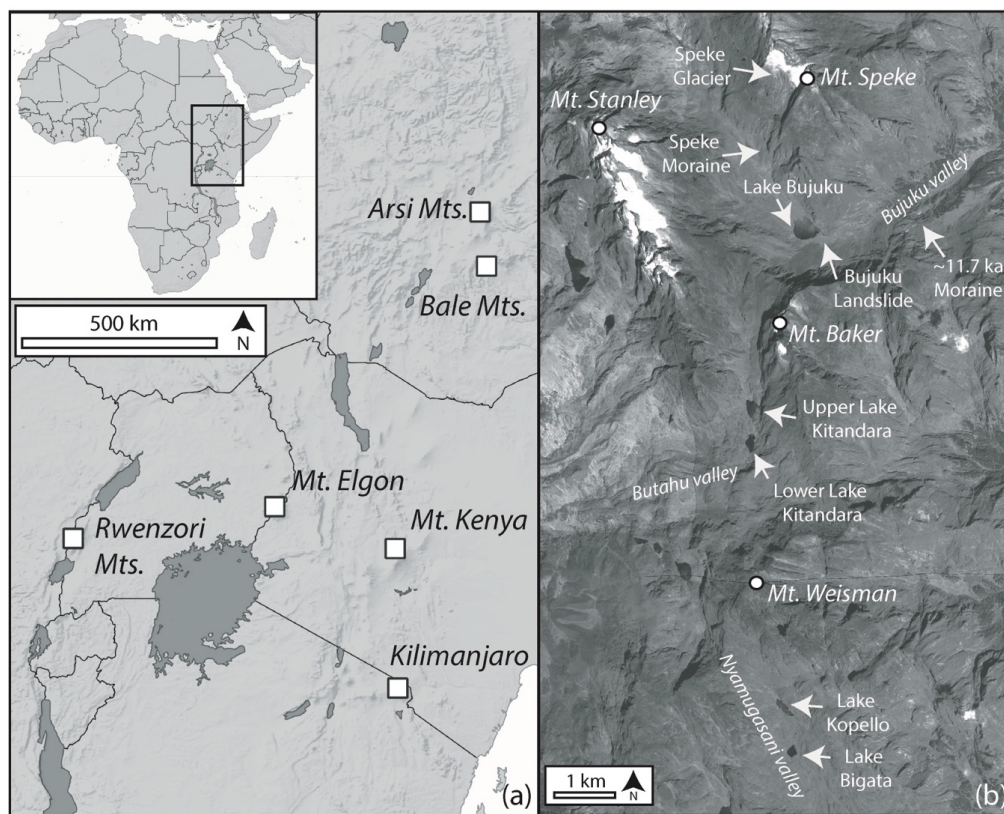


Figure 1. Tropical East Africa and the Rwenzori Mountains. (a) The Rwenzori Mountains, Kilimanjaro, and Mt. Kenya are the only three still-glacierized sites in East Africa. Mt. Elgon in Uganda and the Arsi and Bale Mountains in Ethiopia also host glacial deposits, though are no longer glacierized. (b) Worldview-1 satellite image of the central Rwenzori massif and locations mentioned in the text. Glaciers persist in the Rwenzori on Mt. Stanley, Mt. Speke, and Mt. Baker. Although no longer glacierized, the former Thomson Glacier occupied the peak of Mt. Weisman during the early 20th century.

2 Background

The Rwenzori Mountains are an uplifted horst of crystalline bedrock and are an extreme example of rift shoulder uplift (McConnell et al., 1953; Ring, 2008). Mt. Stanley, the highest point in the range, reaches an elevation of 5,109 meters above sea level (m asl) and, with Mt. Speke and Mt. Baker, is one of three still-glacierized peaks in the Rwenzori (Figure 1). The first quantitative observations of Rwenzori glaciers were made in the early 20th century (Abruzzi,



95 1907). Rwenzori glaciers have retreated markedly since then, decreasing in area from ~6.5 to
96 0.96 km² between 1906 and 2003 CE and losing an estimated 50% of their areal extent between
97 1987 and 2003 CE (Taylor et al., 2006). Modern glaciers in the Rwenzori occur only above
98 ~4,400 m asl and are predicted to disappear within the coming decades (Kaser and Osmaston,
99 2002; Taylor et al., 2006).

100 Although at present glaciers occupy only the highest peaks (Figure 1), the Rwenzori host
101 glacial deposits that attest to more extensive glaciation during and since the last ice age.
102 Osmaston (1965; 1989) grouped moraines in the Rwenzori into distinct glacial stages based on
103 their relative weathering, stratigraphic position, and morphology. The ‘Omurubaho’ stage
104 moraines occur at elevations ~3,600–4,000 m asl and feature ~3–30 m relief above the valley
105 floors (Osmaston, 1989). Osmaston (1989) estimated these moraines to have been deposited
106 during the Early Holocene. Recent ¹⁰Be dating of Omurubaho stage moraines in the Bujuku and
107 Nyamugasani valleys indicates deposition during late-glacial (~15.0–11.7 ka) and Early
108 Holocene time (Jackson et al., in review). The ‘Lac Gris’ stage moraines (Osmaston, 1989) are
109 located up valley and stratigraphically inboard of the Omurubaho stage moraines. Lac Gris stage
110 moraines are predominantly low-relief features (1–2 m above the valley floors) and are within
111 ~100 m of observed 1906 CE ice extents (Abruzzi, 1907). Osmaston (1989) estimated Lac Gris
112 stage moraines to be ~700–100 years old. Based on lichenometry, Bergström (1955) suggested
113 that Lac Gris stage moraines observed near the margin of Elena Glacier on Mt. Stanley date to
114 ~1750 CE. However, the rate at which lichens colonize rock surfaces in the Rwenzori is
115 unconstrained (Osmaston et al., 1989) and the ultimate age of pre-observation Lac Gris moraines
116 remains undetermined.



Livingstone (1967) obtained radiocarbon ages of lake sediments that provide minimum limits on the timing of deglaciation at several locations in the Rwenzori. In the Butahu valley, dated organic sediments within a horizon roughly one meter above presumed basal silts in Upper Lake Kitandara (4,000 m asl; Figure 1) yield a radiocarbon age of ~ 7.7 cal kyr BP (Livingstone, 1967). This provides a minimum-limiting age for glacial recession past this location in the valley. In the Bujuku valley, one radiocarbon age from a layer of gravel-rich peat in a sediment core from Lake Bujuku (3,920 m asl) yields an age of ~ 3.1 cal kyr BP (Livingstone et al, 1967). However, this core did not recover the complete sedimentary succession from the lake and, therefore, may significantly postdate the onset of post-glacial sedimentation in the lake. Rwenzori glacial fluctuations that occurred between the Early Holocene and the (near) historical period are largely unconstrained. A sediment core from Lower Lake Kitandara ($\sim 4,000$ m asl) indicates changes in lake water chemistry at the turn of the 18th century consistent with greater glacier meltwater flux to the lake, although with no corresponding changes in pollen or diatom assemblages (McGlynn et al., 2010). High-resolution analyses of clastic sediment input to numerous Rwenzori alpine lakes indicate that recent historical glacial recession began about 1870 CE (Russell et al., 2009).

Evidence from elsewhere in tropical East Africa suggests that glaciers across the region were near or inboard of their maximum Late Holocene extents for much of Holocene time. Radiocarbon ages from lake sediments in the Bale Mountains and on Mt. Arsi in the Ethiopian Highlands, as well as from Mt. Elgon in Uganda, indicate that glaciers at these sites were inboard of their late-glacial extents, and perhaps had ablated completely, by the Early Holocene (Hamilton and Perrot, 1982; Tiercelin et al., 2008). In Tanzania, the persistence of Holocene ice cover on Kilimanjaro is a subject of ongoing debate. Multiple studies show that the Kilimanjaro



140 Ice Cap has become less extensive over the last ~1 ka, although whether the ice cap may have
141 ablated completely at some point during the Holocene and later re-nucleated is uncertain
142 (Thompson et al., 2002; Kaser et al., 2010; Thompson et al., 2011; Noell et al., 2014). Recent
143 radiocarbon dating of dust and soil horizons within the ice cap suggests a period of net ice cap
144 ablation occurred prior to ~4 ka, followed by net accumulation during the Late Holocene that
145 persisted until near-historical time when recent recession began (Gabielli et al., 2014).

146 At Mt. Kenya, chlorine-36 (^{36}Cl) surface-exposure dating of moraines and glacially
147 molded bedrock in the Teleki Valley indicates that glaciers retreated from their Early Holocene
148 maximum extents by ~10 ka and that the modern Lewis Glacier reached its maximum Late
149 Holocene extent ~200 years ago (Shanahan and Zreda, 2000). In contrast to the existing evidence
150 for limited Middle Holocene glacial expansion in the Rwenzori and on Kilimanjaro, radiocarbon
151 ages of Mt. Kenya's Naro Moru Tarn moraine dam, located ~250 m down valley of the ~200
152 year old Lewis Glacier moraine, suggest a glacial advance occurred in the Teleki Valley between
153 ~6.9 and 4.7 cal yr BP (Johansson and Holmgren, 1985; Karlen et al., 1999). Although disputed
154 (Mahaney et al., 1989), radiocarbon ages from Thomson Tarn in the Hogley Valley also suggest
155 a Middle Holocene glacial advance on Mt. Kenya between ~7.1 and 6.2 cal yr BP (Perrot, 1982).
156 In addition, clastic sediment fluxes to high alpine lakes on Mt. Kenya indicate more dynamic,
157 erosive glacial activity after ~5 cal yr BP (Karlen et al., 1999), although the extent of
158 corresponding glacial margins throughout this period is not known.

159 This study aims to establish the timing of Holocene glacial fluctuations in the Rwenzori
160 Mountains and compare directly the Holocene Rwenzori glacial chronology with records of
161 glaciation and paleoclimate elsewhere in tropical East Africa. Prior work mapping and dating
162 Last Glacial Maximum (LGM) and late-glacial Rwenzori glacial deposits lends crucial temporal



163 and spatial context for the Holocene chronology (Kelly et al., 2014; Jackson et al., 2019; Jackson
164 et al., in review) and allows a more robust comparison of the Rwenzori glacial record with
165 records of past regional climate conditions.

166

167 **3 Study Sites**

168 We focused our study within the Bujuku and Nyamugasani valleys, two independent
169 catchments in the Rwenzori that contain Holocene-age glacial deposits amenable for ^{10}Be dating
170 and for which there is pre-existing numerical age control on pre- or Early Holocene glacial
171 deposits (Jackson et al., 2019; Jackson et al., in review).

172

173 **3.1 Bujuku valley**

174 The modern Speke Glacier occupies the south-facing peak of Mt. Speke (4,890 m asl)
175 near the head of the Bujuku valley (Figure 1, 2). Although today the glacial terminus occurs at
176 ~4,600 m asl, in 1958 CE the glacier extended down slope to ~4,350 m asl (Whittow et al.,
177 1963). Lac Gris stage deposits occur on Mt. Speke between ~4,000 and 4,500 m asl (Osmaston,
178 1989), including a Lac Gris stage moraine ~300 m downslope from the 1958 CE glacial extent
179 (Osmaston, 1989)(Figure 2). Observations by Abruzzi (1907) indicate that ice had abandoned
180 this Lac Gris stage moraine prior to 1906 CE, though the precise timing of retreat is not known
181 (Whittow, 1963).

182 Omurubaho stage moraines occur ~2.5 km down the Bujuku valley from the Lac Gris
183 stage moraines, and the innermost (i.e., farthest up valley) of these dates to ~11.7 ka (Jackson et
184 al., in review). There are no moraines in the valley between the ~11.7 ka moraine and the Lac
185 Gris stage deposits on Mt. Speke. Approximately 1.5 km up valley from the ~11.7 ka moraine,



186 the outlet of Lake Bujuku is dammed by a landslide that originated on the north-facing slope of
187 Mt. Baker (Figure 1). This landslide is dated to ~11 ka and shows no evidence of having been
188 impeded or reworked by ice either during or subsequent to deposition (Cavagnaro, 2017).
189 Therefore, it is likely that the landslide was emplaced after ice retreated up valley and the age
190 (~11 ka) is a minimum-limiting age for deglaciation of the valley floor at this location (Jackson
191 et al., in review).

192

193 **3.2 Nyamugasani valley**

194 Mt. Weisman (4,620 m asl) marks the head of the Nyamugasani valley (Figure 1, 2).
195 Although no longer glacierized, the former Thomson Glacier occupied a cirque on the south-
196 facing slope of the peak until the mid-20th century (Osmaston and Pasteur, 1972). Omurubaho-
197 stage moraines occur in the Nyamugasani valley between ~3,800 and 4,000 m asl. The innermost
198 (i.e., farthest up valley) Omurubaho moraine is dated to ~11.2 ka and dams Lake Bigata (~4,000
199 m asl)(Jackson et al., in review). There are no moraines between Lake Bigata and the peak of Mt.
200 Weisman, although glacially transported boulders are ubiquitous on the valley
201 floor. Approximately 0.5 km up valley from the ~11.2 ka moraine, four boulders on a bedrock
202 rise at the outlet of Lake Kopello (~4,020 m asl) yield ages between ~12.1 and 10.5 ka,
203 indicating continued recession of ice in the valley after ~11 ka (Jackson et al., in review).

204

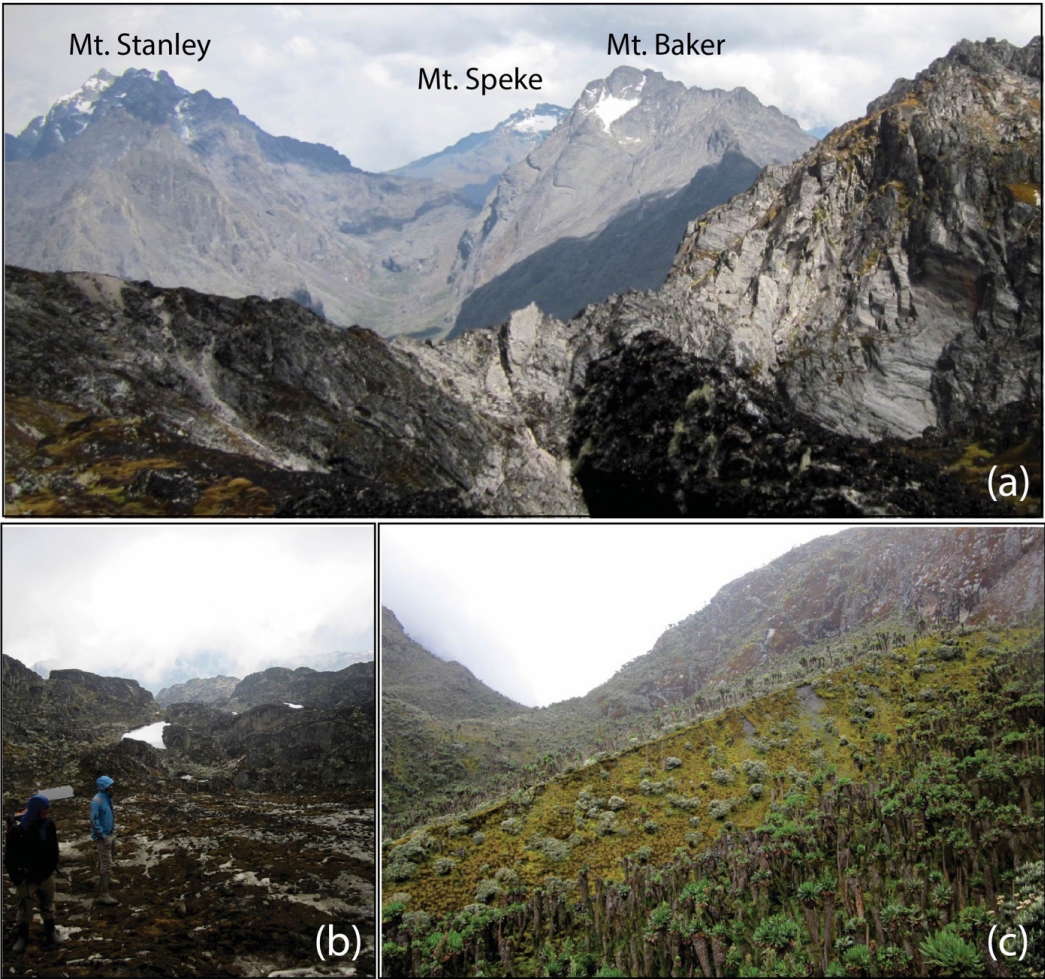


Figure 2. Glacial features in the central Rwenzori Mountains. (a) A view toward the north from the peak of Mt. Weisman. Mt. Stanley, Mt. Speke, and Mt. Baker are the three still-glacierized peaks in the Rwenzori. Above 4,000 m asl, the Rwenzori are dominated by bare bedrock with some lichen and moss cover. (b) A view down valley, toward the south, from the unoccupied cirque on Mt. Weisman that once held the former Thomson Glacier. (c) The right-lateral Speke moraine beneath Speke Glacier features a sharp crest and steep ice-proximal slope. View is toward the east.



216 4 Methods

217 We conducted three field seasons in the Rwenzori between 2012 and 2016. While in the
 218 field we classified glacial-geomorphic features based on their morphology, stratigraphic position,
 219 and degree of weathering and mapped these features onto WorldView-1 0.5-m resolution
 220 satellite imagery. We collected samples for ^{10}Be dating from boulders on moraines, boulders on
 221 bedrock, and from bedrock surfaces using a hammer and chisel and the drill-and-blast method of
 222 Kelly (2003). We took care to sample boulders that showed no indication of post-depositional
 223 movement and, where possible, surfaces with no dip in order to minimize topographic shielding
 224 correction uncertainties. We recorded sample locations with a handheld GPS (± 3 m vertical, ± 1
 225 m horizontal), determined topographic shielding using a clinometer, and measured sample
 226 surface dip and dip direction, if applicable, with a handheld compass (Table 1).

227

Table 1: Rwenzori Sample Information												
Bujuku Valley												
Map ID	Sample ID	Landform	Latitude (DD)	Longitude (DD)	Elev. (m)	Atm.	Thickness (cm)	Density (g/cm ³)	Shielding	Erosion (mm/yr)	$^{10}\text{-Be}$ (atoms/g)	\pm $^{10}\text{-Be}$ (atoms/g)
1	RZ-12-21	Speke moraine	0.38750	29.88821	4095	std	1.5	2.65	0.909	0	9.29E+03	7.84E+02
2	RZ-12-22	Speke moraine	0.38768	29.88816	4046	std	1.2	2.65	0.909	0	6.96E+03	4.80E+02
3	RZ-12-24	Speke moraine	0.38768	29.88816	4046	std	1.3	2.65	0.909	0	1.02E+04	5.07E+02
4	RZ-12-25	Speke moraine	0.38768	29.88816	4046	std	1.5	2.65	0.909	0	1.17E+04	3.87E+02
Nyamugasani Valley												
Map ID	Sample ID	Landform	Latitude (DD)	Longitude (DD)	Elev. (m)	Atm.	Thickness (cm)	Density (g/cm ³)	Shielding	Erosion (mm/yr)	$^{10}\text{-Be}$ (atoms/g)	\pm $^{10}\text{-Be}$ (atoms/g)
5	RZ-15-10	Perched boulder	0.32265	29.89128	4397	std	4.0	2.65	0.976	0	3.78E+05	3.56E+03
6	RZ-15-11	Perched boulder	0.32263	29.89132	4400	std	2.0	2.65	0.976	0	3.60E+05	2.50E+03
7	RZ-15-09	Perched boulder	0.32385	29.89034	4431	std	3.0	2.65	0.983	0	3.51E+05	3.79E+03
8	RZ-15-07	Perched boulder	0.32589	29.88928	4488	std	1.9	2.65	0.989	0	1.51E+05	1.50E+03
9	RZ-15-08	Perched boulder	0.32601	29.88953	4498	std	2.0	2.65	0.99	0	2.19E+05	4.14E+03
10	RZ-15-01	Cirque Bedrock	0.32793	29.88877	4509	std	1.9	2.65	0.969	0	1.66E+05	1.81E+03
11	RZ-15-02	Cirque Bedrock	0.32786	29.88887	4526	std	1.4	2.65	0.97	0	1.69E+05	1.84E+03
12	RZ-15-03	Cirque Bedrock	0.32781	29.88871	4536	std	2.8	2.65	0.97	0	1.89E+05	1.68E+03

228

229 **Table 1.** Geographic data and sample characteristic information for Rwenzori samples.

230



We isolated beryllium from each sample and associated process blanks at the Dartmouth College Cosmogenic Nuclide Laboratory using a modified version of the methods described in Schaefer et al. (2009). All $^{10}\text{Be}/^9\text{Be}$ ratios were measured at the Lawrence Livermore Center for Accelerator Mass Spectrometry and normalized to the 07KNSTD3110 standard (Nishiizumi et al., 2007)(Table 2). ^{10}Be ages presented in Figures 3-5 and in Table 3 are as calculated using version 3 of the online calculator described by Balco et al. (2008 and subsequently updated) with a high-altitude, low-latitude production rate (Kelly et al., 2015) and time-invariant scaling framework (“St” scaling; Lal, 1991; Stone, 2000). We present ^{10}Be ages calculated using an alternative, time-variant scaling framework (“LSDn” scaling; Lifton et al., 2016) in Table 3. Our choice of scaling framework does not alter our overall interpretations. Where ^{10}Be concentrations are of bedrock rather than glacially deposited sediments, we report the nuclide concentration rather than the exposure-age equivalent (Figure 4, Table 1), as bedrock nuclide concentrations may reflect multiple periods of exposure rather than a single exposure duration.

Table 2: Rwenzori Sample Chemistry

Bujuku Valley											
Map ID	Sample ID	Landform	Cathode ID	Quartz (g)	Carrier wt. (mg)	Carrier Conc. (ppm)	Sample ($^{10}\text{Be}/^9\text{Be}$)	\pm Sample ($^{10}\text{Be}/^9\text{Be}$)	Process Blank Cathode ID	Blank ($^{10}\text{Be}/^9\text{Be}$)	\pm Blank ($^{10}\text{Be}/^9\text{Be}$)
1	RZ-12-21	Speke moraine	BE43754	16.1727	0.2013	0.973	1.14775E-14	9.69152E-16	BE43758	1.63761E-15	3.53685E-16
2	RZ-12-22	Speke moraine	BE43755	32.3243	0.2006	0.973	1.72402E-14	1.19007E-15	BE43758	1.63761E-15	3.53685E-16
3	RZ-12-24	Speke moraine	BE43756	23.8116	0.2013	0.973	1.85318E-14	9.2237E-16	BE43758	1.63761E-15	3.53685E-16
4	RZ-12-25	Speke moraine	BE43757	40.0454	0.2010	0.973	3.59382E-14	1.18435E-15	BE43758	1.63761E-15	3.53685E-16
Nyamugasani Valley											
Map ID	Sample ID	Landform	Cathode ID	Quartz (g)	Carrier wt. (mg)	Carrier Conc. (ppm)	Sample ($^{10}\text{Be}/^9\text{Be}$)	\pm Sample ($^{10}\text{Be}/^9\text{Be}$)	Process Blank Cathode ID	Blank ($^{10}\text{Be}/^9\text{Be}$)	\pm Blank ($^{10}\text{Be}/^9\text{Be}$)
5	RZ-15-10	Perched boulder	BE39810	100.945	0.0907	1.338	4.70348E-12	4.43266E-14	BE39812	3.81273E-15	6.15885E-16
6	RZ-15-11	Perched boulder	BE39811	102.028	0.091	1.338	4.51587E-12	3.13429E-14	BE39812	3.81273E-15	6.15885E-16
7	RZ-15-09	Perched boulder	BE39809	100.573	0.0916	1.338	4.30701E-12	4.65808E-14	BE39812	3.81273E-15	6.15885E-16
8	RZ-15-07	Perched boulder	BE39808	101.292	0.0881	1.338	1.94507E-12	1.93123E-14	BE39812	3.81273E-15	6.15885E-16
9	RZ-15-08	Perched boulder	BE40319	12.014	0.1650	1.340	1.78244E-13	3.36358E-15	BE40308	7.21905E-16	1.41075E-16
10	RZ-15-01	Cirque Bedrock	BE39531	100.57	0.0961	1.337	1.94043E-12	2.11829E-14	BE39534	6.99989E-15	5.814E-16
11	RZ-15-02	Cirque Bedrock	BE39532	100.79	0.0967	1.337	1.97014E-12	2.14812E-14	BE39534	6.99989E-15	5.814E-16
12	RZ-15-03	Cirque Bedrock	BE39533	101.33	0.0930	1.337	2.30326E-12	2.04419E-14	BE39534	6.99989E-15	5.814E-16

Table 2. Processing data and sample chemistry for all Bujuku and Nyamugasani valley samples.



248 We do not correct ^{10}Be ages for the potential impacts of snow cover or vegetation. Snow
249 does not persist for considerable lengths of time at the sample elevations due to warm daytime
250 temperatures and intense solar radiation. Vegetation in the Rwenzori Mountains above ~4,000 m
251 asl is sparse (Osmaston and Pasteur, 1972; Foster et al., 2001) and all samples were collected
252 above this elevation. Some samples featured a patchy cover of lichen or moss (≤ 2 cm thick) and
253 we avoided this where possible, although we note that a persistent cover of moss of 2 cm
254 thickness would alter the resultant exposure ages by $< 2\%$ (Dunai, 2010; Plug et al., 2007). We
255 also did not correct ^{10}Be ages for the potential influence of erosion, as samples did not show
256 evidence that could be used to estimate quantitatively surface erosion rates. Previous applications
257 of ^{10}Be dating in the Rwenzori suggest that raised quartz veins and rock surfaces on single
258 moraine crests yield statistically similar ages (Jackson et al., 2019).

259

260

261

262



Table 3: Rwenzori Surface-Exposure Ages

Bujuku Valley								
Map ID	Sample ID	Landform	Age (St)	± (int; St)	± (ext; St)	Age (LSDn)	± (int; LSDn)	± (ext; LSDn)
1	RZ-12-21	Speke moraine	360	30	40	370	30	40
2	RZ-12-22	Speke moraine	270	20	20	280	20	30
3	RZ-12-24	Speke moraine	400	20	30	410	20	30
4	RZ-12-25	Speke moraine	460	20	30	480	20	30
Nyamugasani Valley								
Map ID	Sample ID	Landform	Age (St)	± (int; St)	± (ext; St)	Age (LSDn)	± (int; LSDn)	± (ext; LSDn)
5	RZ-15-10	Perched boulder	12130	120	690	11510	110	680
6	RZ-15-11	Perched boulder	11360	80	650	11010	80	640
7	RZ-15-09	Perched boulder	10920	120	630	10700	120	630
8	RZ-15-07	Perched boulder	4520	50	260	4980	50	290
9	RZ-15-08	Perched boulder	6520	120	390	6590	130	400
10	RZ-15-01	Cirque Bedrock	5010	60	290	5400	60	320
11	RZ-15-02	Cirque Bedrock	5040	60	290	5430	60	320
12	RZ-15-03	Cirque Bedrock	5680	50	320	5930	50	350

Table 3. Cosmogenic ^{10}Be surface-exposure ages for samples from the Bujuku and Nyamugasani valleys. We report ages as calculated using both time-invariant (“St”; Lal, 1991; Stone, 2000) and time-variant (“LSDn”; Lifton et al., 2016) scaling with internal (“int”) and external (“ext”) error.

5 Results

5.1 Bujuku valley

We term the prominent Lac Gris stage moraine on the south-facing slope of Mt. Speke the ‘Speke moraine’ (Figures 2-3). The Speke moraine marks the first glacial deposit up valley of the Omurubaho-stage moraine dated to ~11.7 ka (Jackson et al., in review) and is ~300 m elevation downslope from the 1958 CE glacier extent (Whittow, 1963). The Speke moraine is also ~1.5 km up valley of the ~11.0 ka landslide that dams Lake Bujuku (Cavagnaro, 2017). The right- and left-lateral ridges of the Speke moraine are well preserved and have steep ice-contact slopes with more fan-like, low-angle ice-distal slopes. Four samples from the right-lateral ridge yield ^{10}Be ages between ~0.46 and 0.27 ka (RZ-12-21, 22, 24, 25; ~4,050 m asl)(Table 1).

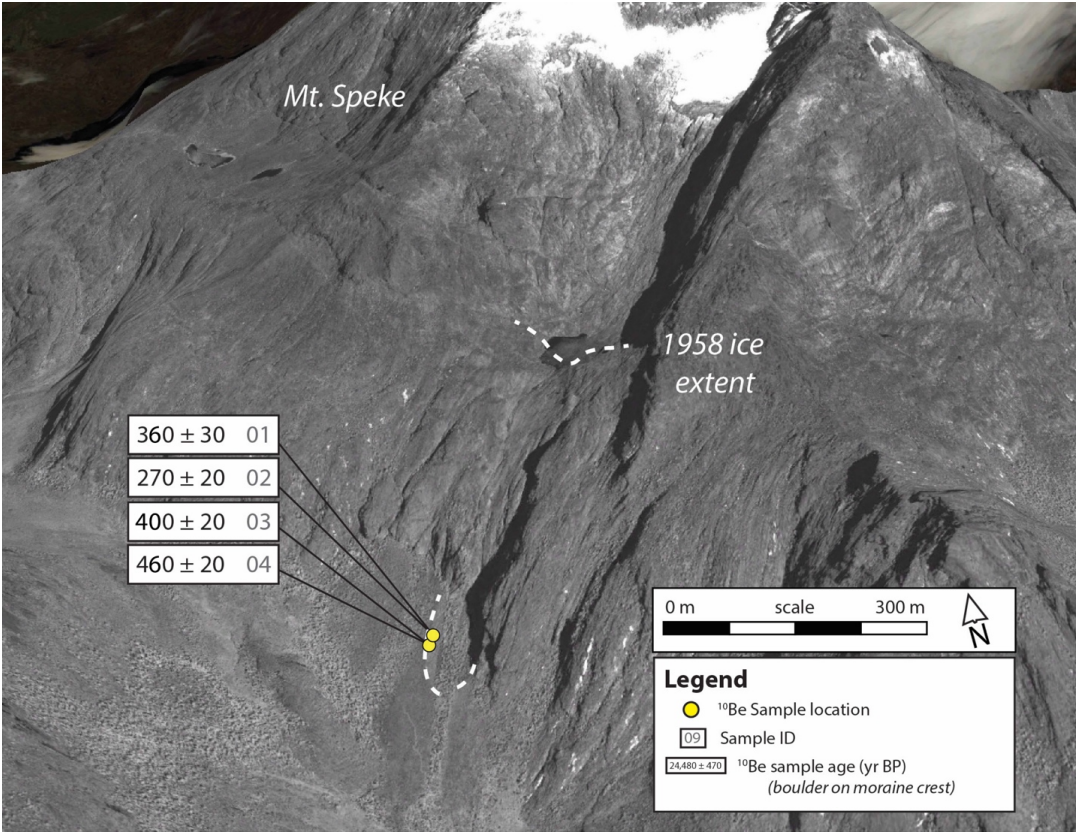


Figure 3. Mount Speke and ^{10}Be ages of the Speke moraine. Ages are shown in black with internal analytical uncertainties. Sample ID numbers as in Tables 1-3 are shown in grey. The ice-contact slope of the Speke moraine is outlined in dashed white, as is the documented 1958 ice margin ~ 300 m upslope (Whittow et al., 1963). Sample locations are mapped onto a 0.5 m-resolution Worldview-1 satellite image.

5.2 Nyamugasani valley

We dated five boulders on bedrock along an elevation transect on the south-facing slope of Mt. Weisman (Figure 4, Tables 1-3). The transect extends from ~4,400 to 4,490 m asl. All samples are from glacially molded, sub-rounded boulders except for sample RZ-15-08 which is from an angular boulder. Based on their size and position on the slope (i.e., away from the valley walls where rockfall may occur), we presume these boulders were deposited by a receding glacier. The two most down valley samples yield ^{10}Be ages of 12.1 ± 0.1 ka (RZ-15-10; 4,397m



291 asl) and 11.4 ± 0.1 ka (RZ-15-11; 4,400 m asl). A third sample is located ~170 m up valley at
292 ~4,430 m asl and dates to 10.9 ± 0.1 ka (RZ-15-09). Approximately 250 m farther up valley at
293 ~4,490 m asl, two boulders on bedrock knobs yield ages of 4.5 ± 0.0 ka (RZ-15-07) and 6.5 ± 0.1
294 ka (RZ-15-08).

295 In addition to the elevation transect of boulders on bedrock, we measured ^{10}Be
296 concentrations in three samples of the bedrock floor of the unoccupied cirque below the peak of
297 Mt. Weisman (4,509-4,536 m asl)(Figures 2, 4). We term this feature the 'Thomson cirque'. The
298 bedrock samples from Thomson cirque contain ^{10}Be concentrations between 1.94 and 2.03×10^{-12}
299 atoms/gram (quartz), equivalent to ~5.0-5.7 thousand years of exposure (RZ-15-01, 02,
300 03)(Table 1, 3).

301

302

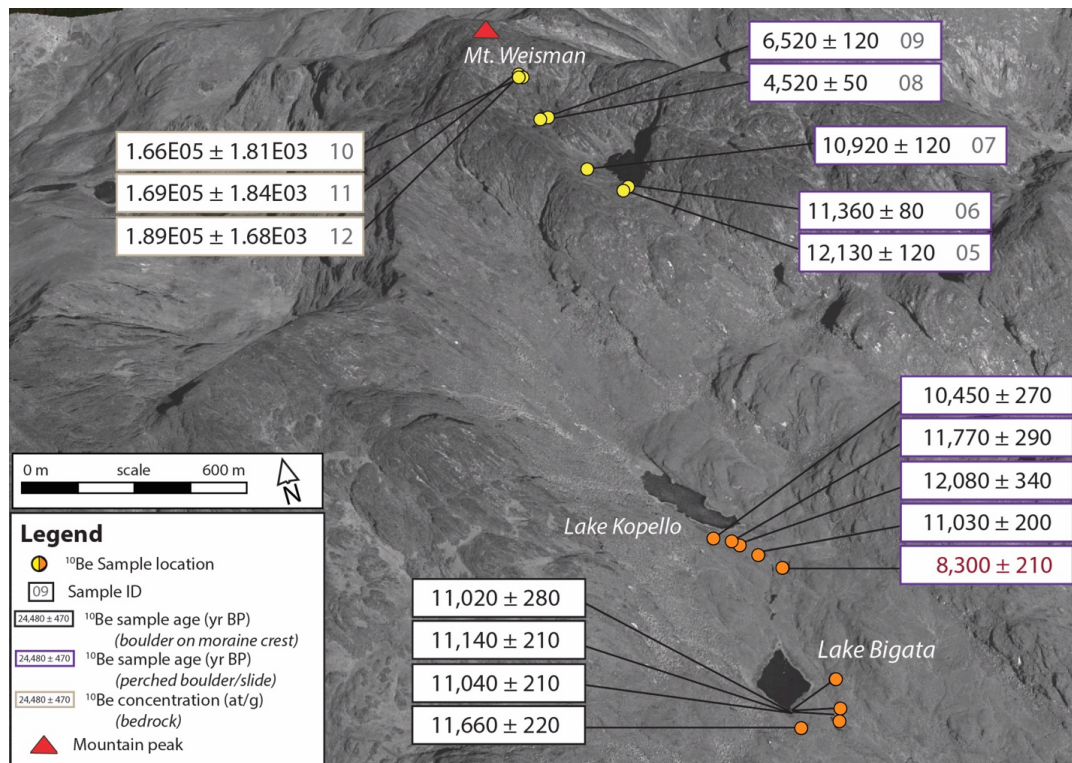


Figure 4. ^{10}Be ages and concentrations in the Nyamugasani valley. Ages are shown in black with internal analytical uncertainties. Sample ID numbers as in Tables 1-3 are shown in grey. Sample locations are marked by yellow circles and mapped onto a 0.5-m resolution Worldview-1 satellite image. Previously reported ^{10}Be ages from the moraine that dams Lake Bigata and from boulders on bedrock near the outlet of Lake Kopello are marked with orange circles (Jackson et al., in review). Ages considered to be outliers are shown in red.

6 Discussion

6.1 Holocene Glacial Fluctuations in the Rwenzori Mountains

The ^{10}Be ages from the Bujuku and Nyamugasani valleys suggest that glaciers in both catchments retreated rapidly during the Early Holocene. Based on the lack of glacial deposits in the Bujuku valley between the ~ 11.7 ka moraine and the Speke moraine, and the ~ 11.0 ka age of the landslide that dams Lake Bujuku (Cavagnaro, 2017), we suggest that the former Bujuku valley glacier retreated up the valley at, or shortly after, the onset of the Holocene. The landslide occurs ~ 1.5 km up valley of the ~ 11.7 ka moraine and is undisturbed, indicating that ice had



318 retreated at least this distance up valley by ~11 ka and that ice remained up valley of this site
319 throughout the Holocene. Although it is possible that wetland or colluvium deposits on the valley
320 floor buried additional glacial deposits, there are no lateral moraines higher on the valley walls
321 and no evidence of glacial readvance over these colluvial sediments.

322 The morphology of the Speke moraine in the Bujuku valley, with steep ice-contact slopes
323 and more gentle ice-distal slopes (Figure 2), indicates that the lateral ridges formed as rock-fall
324 debris from the slopes of Mt. Speke fell onto the former Speke Glacier surface and was
325 transported supraglacially to the ice margin. The deposition of this rock-fall debris along the
326 glacier margins produced the fan-like ice-distal slopes of the Speke moraine. Deposition ceased
327 when the glacier receded and the moraine was abandoned at ~270-460 years ago.

328 Additional evidence for Early Holocene glacial recession in the Rwenzori comes from the
329 Nyamugasani valley. The stratigraphically innermost moraine (i.e., farthest up valley) in the
330 Nyamugasani valley dates to ~11.2 ka (Jackson et al., in review) (Figure 4). Approximately 0.5
331 km farther up valley, four boulders on a bedrock rise that dams Lake Kopello yield ages between
332 ~12.1 and 10.5 ka (Jackson et al., in review). An additional ~1.6 km up valley from the Lake
333 Kopello bedrock, glacially-transported boulders set down on bedrock yield ages between ~12.1
334 and 10.9 ka. Based on the statistical similarity of these sample ages, we interpret these samples
335 to reflect rapid glacier recession from the innermost Nyamugasani valley moraine (~11.2 ka)
336 during the Early Holocene. These data suggest that the valley was deglaciated to an elevation of
337 ~4,430 m asl by at least ~10.9 ka.

338 Farther up valley, bedrock on the floor of Thomson cirque, below the south-facing peak
339 of Mt. Weisman, has ¹⁰Be concentrations equivalent to ~5.0-5.7 ka of net exposure (Figure 4).
340 The cirque was occupied by the former Thomson Glacier until at least the mid 20th century



(Meador, 1937; Whittow et al., 1963; Osmaston and Pasteur, 1972). This implies that the cirque was ice-free for some period of time before its occupation by Thomson Glacier (Doughty et al., in press). If we assume that ice cover during the LGM (Kelly et al., 2014; Jackson et al., 2019) was erosive enough to remove any pre-existing ^{10}Be from the bedrock surface, the measured bedrock ^{10}Be concentrations reflect the total period of exposure of the bedrock (i.e., ice-free conditions) after the LGM. More specifically, based on the Early Holocene age of moraines down valley (Jackson et al., in review), we suggest the Thomson cirque bedrock ^{10}Be concentrations indicate the net duration of bedrock exposure (~ 5.0 - 5.7 ka) during the Holocene.

This interpretation, and the observation that the cirque was occupied by Thomson Glacier during the early and middle 20th century, leads to one notable consequence. Namely, if the Thomson cirque was ice-free for ~ 5.0 - 5.7 kyr during the Holocene yet occupied by ice during at least a portion of Late Holocene time, this implies that ice had ablated away completely in the cirque at some point earlier in the Holocene before re-nucleating prior to the 20th century. This scenario may include multiple periods of glacial ablation and readvance, or a single period of ice-free conditions followed by Late Holocene re-nucleation. Although the timing of ice recession and re-nucleation within the cirque cannot be established with the data presented here, the bedrock ^{10}Be concentrations suggest that the cirque remained ice-free for a significant portion of the Holocene Epoch.

The two boulders on bedrock ~ 10 - 20 m downslope of the cirque (dated to ~ 4.5 and 6.5 ka; RZ-15-07, 08) suggest that the former Thompson Glacier extended to this downslope location during the Middle Holocene. However, the ^{10}Be ages of these boulders are similar to the exposure-age equivalent of the nearby cirque bedrock (~ 5.0 - 5.7 ka), which suggests that the boulders may contain inherited ^{10}Be . In this scenario, the boulders would have been plucked



364 from the nearby cirque floor and transported a short distance (~100 m) by the former Thomson
365 Glacier during a Late Holocene readvance. Alternatively, the boulders may have fallen onto the
366 ice surface from the valley walls above and escaped sub-glacial erosion prior to deposition.
367 Sample RZ-15-08 (~6.5 ka) is from an angular boulder, which may indicate that it was
368 transported supraglacially after falling onto the former ice surface from the valley headwall. In
369 contrast, sample RZ-15-07 (~4.5 ka) was sub-rounded in appearance and so was presumably
370 eroded during glacial transport. These sampled boulders are located near the early-20th century
371 snow or ice margin, as shown in photographs from 1937 CE (Meader, 1937). The proximity of
372 the samples to the early 20th century snow/ice margin supports the interpretation that the boulders
373 were deposited during a Late Holocene advance of Thomson Glacier, but more data are needed
374 to determine the depositional histories of these samples. Due to the uncertainties associated with
375 these samples, we do not use their ¹⁰Be ages in any subsequent interpretations.

376 Overall, ¹⁰Be ages from the Bujuku and Nyamugasani valleys suggest glacial recession
377 occurred in both catchments during the Early Holocene and that glaciers in these valleys then
378 retreated to, or inboard of, their maximum late-19th or early-20th century extents (Figure 5). In the
379 Nyamugasani valley, ¹⁰Be concentrations measured in bedrock samples from the floor of
380 Thomson cirque suggest ~5-6 kyr of net exposure of surfaces that were glacierized in the first
381 half of the 20th century. The results do not preclude the possibility that glaciers persisted on the
382 high Rwenzori peaks throughout the Holocene, albeit inboard of their late 19th century positions.
383 However, the data suggest that glaciers in the Bujuku and Nyamugasani valleys did not advance
384 beyond their Late Holocene maximum ice positions during Early or Middle Holocene time.

385

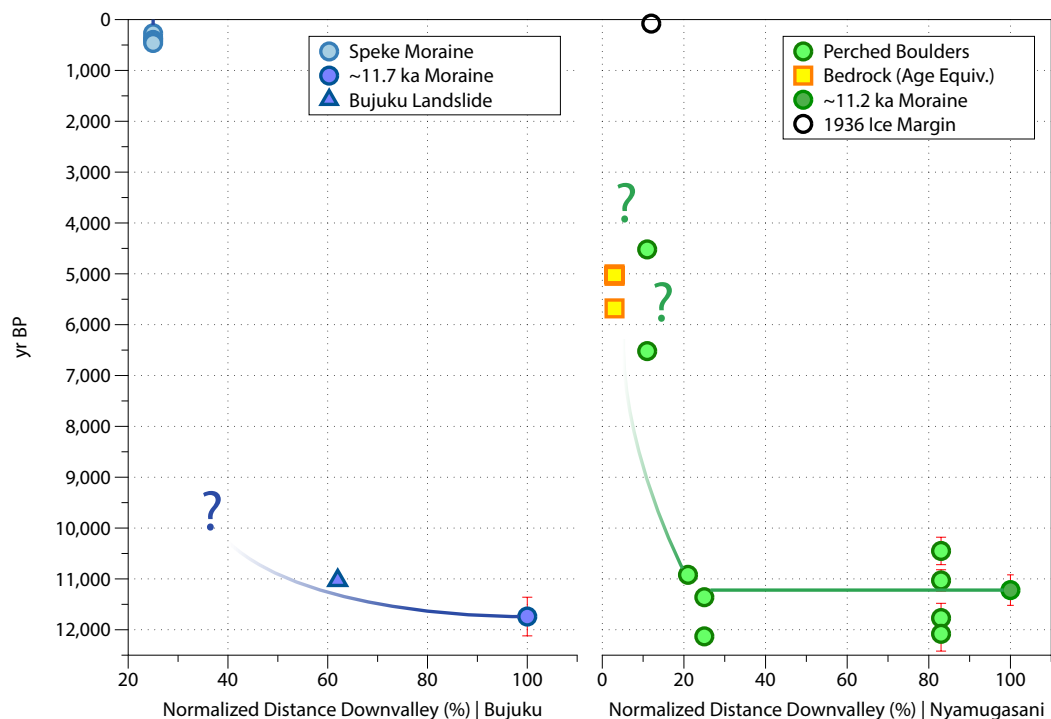


Figure 5. Normalized glacial extent in the Bujuku and Nyamugasani valleys during the Holocene. Lines indicate reconstructed glacial extent, question marks highlight periods where glacial extent is uncertain. (left) In the Bujuku valley, the maximum dated Holocene position (~11.7 ka moraine; Jackson et al., in review) is roughly 1.5 km down valley of the ~11 ka landslide which dams Lake Bujuku (Cavagnaro, 2017) and over 3 km down valley from the Speke moraine. (right) In the Nyamugasani valley, the most up valley moraine in the catchment dates to ~11.2 ka. Boulders set down on the Kopello ridge yield ages between ~12.1-10.5 ka. The Nyamugasani transect boulders yield similar ages to those on the Kopello ridge, but are 1.8 km farther up valley. Yellow squares mark the exposure-age equivalents (^{10}Be concentration) of samples of bedrock from Thomson cirque, although we emphasize that these ages represent the cumulative exposure duration (likely since the LGM), and do not necessarily reflect the most recent period of exposure.

6.2 Patterns of East African Glaciation and Temperature during the Holocene

Although sensitive to precipitation, humidity, aspect, and hypsometry, glaciers in the ‘humid’ inner tropics (~10°N-10°S) are influenced primarily by temperature (e.g., Sagredo et al., 2014). This includes glaciers in the Rwenzori (Taylor et al., 2006; Russell et al., 2009; Kelly et al., 2014; Doughty et al., in press). The hypothesis that glacial fluctuations in the Rwenzori during the Holocene are controlled by temperature is supported by a comparison of our data with



404 paleolimnological records of regional precipitation and temperature (Figure 6). Organic
405 geochemical (branched glycerol dialkyl glycerol tetraethers; brGDGTs) proxy temperature
406 records from four East African lakes and the Congo River Basin indicate temperatures warmed
407 by ~ 1 °C from ~ 12 -11 ka, were similar to Late Holocene values from ~ 11 to 8 ka, and then rose
408 to a mid-Holocene thermal maximum between 6 and 5 ka, before cooling to Late Holocene
409 values (Ivory et al., 2017, and references therein). The Early Holocene is also marked by the
410 African Humid Period (AHP; ~ 11.6 -5.0 ka), a time of elevated precipitation across tropical
411 Africa (Garcin et al., 2007) reflected in precipitation reconstructions from Lakes Victoria and
412 Tanganyika, the Nile River Delta, and at the foot of the Rwenzori Mountains at Lake Edward
413 (Russell et al., 2003a; Buening and Russell, 2004; Tierney et al., 2008; Berke et al., 2012;
414 Weldeab et al., 2014). Declining precipitation associated with the end of the AHP began at ~ 5.2
415 ka in western Uganda, recorded by rising salinity in Lake Edward (Russell et al., 2003b, Russell
416 and Johnson, 2006), roughly coincident with the onset of cooling in East Africa. Rwenzori
417 glaciers thus retreated during a wet and warming Early Holocene and remained near or inboard
418 of their Late Holocene maxima during the warm, drying Middle Holocene. The end of the AHP
419 and the onset of cooler conditions in East Africa broadly coincides with the transition to more
420 erosive glacial margins on Mt. Kenya (Karlen et al., 1999) and with the beginning of extended
421 net accumulation on the Kilimanjaro Ice Cap after ~ 4 ka (Gabielli et al., 2014). We suggest that
422 regional temperatures were sufficiently high during the Early and Middle Holocene to dominate
423 glacial mass balance in the African tropics in spite of elevated precipitation.

424 The pattern of Holocene glacial fluctuations inferred in the Rwenzori is broadly
425 consistent with reconstructed glacial histories from elsewhere in East Africa. In Ethiopia,
426 Uganda, and Kenya, glaciers retreated either during or prior to the Early Holocene (Hamilton and



Perrot, 1982; Shanahan and Zreda, 2000; Tiercelin et al., 2008) and remained near or inboard of reconstructed Late Holocene positions throughout Holocene time. Although disputed (Mahaney, 1989), there is some evidence for a Middle Holocene readvance of glaciers on Mt. Kenya (Perrot, 1982; Johansson and Holmgren, 1985; Karlen et al., 1999). The ages of ~4.5–6.5 ka of perched boulders in the Rwenzori's Nyamugasani valley may indicate a similar Middle Holocene readvance, but to a position near or inboard of the maximum Late Holocene extent (Meador, 1937; Osmaston and Pasteur, 1972). Acknowledging this uncertainty, we suggest that the Rwenzori chronology is generally representative of Holocene glacial fluctuations in tropical Africa.

Our comparison of Rwenzori glacier extents with regional GDGT-based temperature records indicates that ice masses did not respond linearly to temperature. For example, GDGT temperature reconstructions suggest regional temperatures at ~11 ka were similar to temperatures at ~1 ka-present (Ivory et al., 2017). In contrast, glacial margins during the Early Holocene were ~330 m lower in the Nyamugasani valley and ~490 m lower in the Bujuku valley than during the Late Holocene (Figure 6). This difference may be due to the fact that there was more substantial, if retreating, ice volume in the Rwenzori at ~11 ka relative to the Late Holocene, and that Late Holocene ice was re-nucleating or re-advancing after a period of sustained ablation. Alternatively, this difference may reflect two distinct equilibrium glacial mass balances at similar temperatures but with different precipitation regimes and radiative boundary conditions. Modeling suggests that past changes in Rwenzori equilibrium-line altitude are only weakly influenced by precipitation amount, and that the large (~60% increase; Buening and Russell, 2004) changes in precipitation in western Uganda during the AHP are insufficient to explain the large downslope movement of Rwenzori glaciers observed at ~11 ka (Doughty et al., in press).



450 Early Holocene glacial recession is coincident with both increasing atmospheric CO₂ (Monnin et
451 al., 2001)(Figure 6), which increases surface longwave radiation, and with rising mean-annual
452 equatorial insolation after ~10 ka (Berger and Loutre, 1991). Because tropical glaciers undergo
453 ablation throughout the year, mean-annual radiation (both insolation and longwave) influences
454 glacial mass balance in the tropics (Kaser and Osmaston, 2002) and may have played a role in
455 Holocene glacial extents. However glaciers in the Rwenzori and elsewhere in East Africa
456 apparently re-nucleated or readvanced during the Late Holocene, whereas atmospheric CO₂ and
457 mean annual insolation continued to rise. Alternatively, seasonal, rather than mean-annual,
458 insolation is another potential forcing mechanism for tropical glacial fluctuations. The sun passes
459 directly over the equator twice each year in September and March, coincident with the twice-
460 annual equatorial wet season (Sept.-Nov. and March-May) and the passage of the Intertropical
461 Convergence Zone over the equator (Singarayer and Burrough, 2015). Modeling studies of ice
462 cliffs on Kilimanjaro (Mölg et al., 2003a) and of modern Rwenzori glaciers (Mölg et al., 2003b)
463 suggest that a transition to more regionally arid conditions after ~1880 CE reduced cloud cover
464 and increased the amount of net annual solar radiation impacting glacier surfaces during dry
465 seasons, which may have encouraged further ablation after the initiation of recent Rwenzori
466 deglaciation ~1870 CE (Russell et al., 2009). Neither of the Rwenzori dry seasons (June-Aug
467 and Dec-Feb) had insolation minima during Middle Holocene (Figure 6), and so the Late
468 Holocene re-nucleation or readvance of African glaciers is difficult to reconcile with this
469 mechanism. Elevated wet season (Sept.-Nov.) insolation could play a role, but Sept. and March
470 insolation trends counteract each other during the Holocene. More work is needed to determine
471 the discrete influences on glacial mass balance over millennial timescales during the Holocene in
472 the East African tropics.

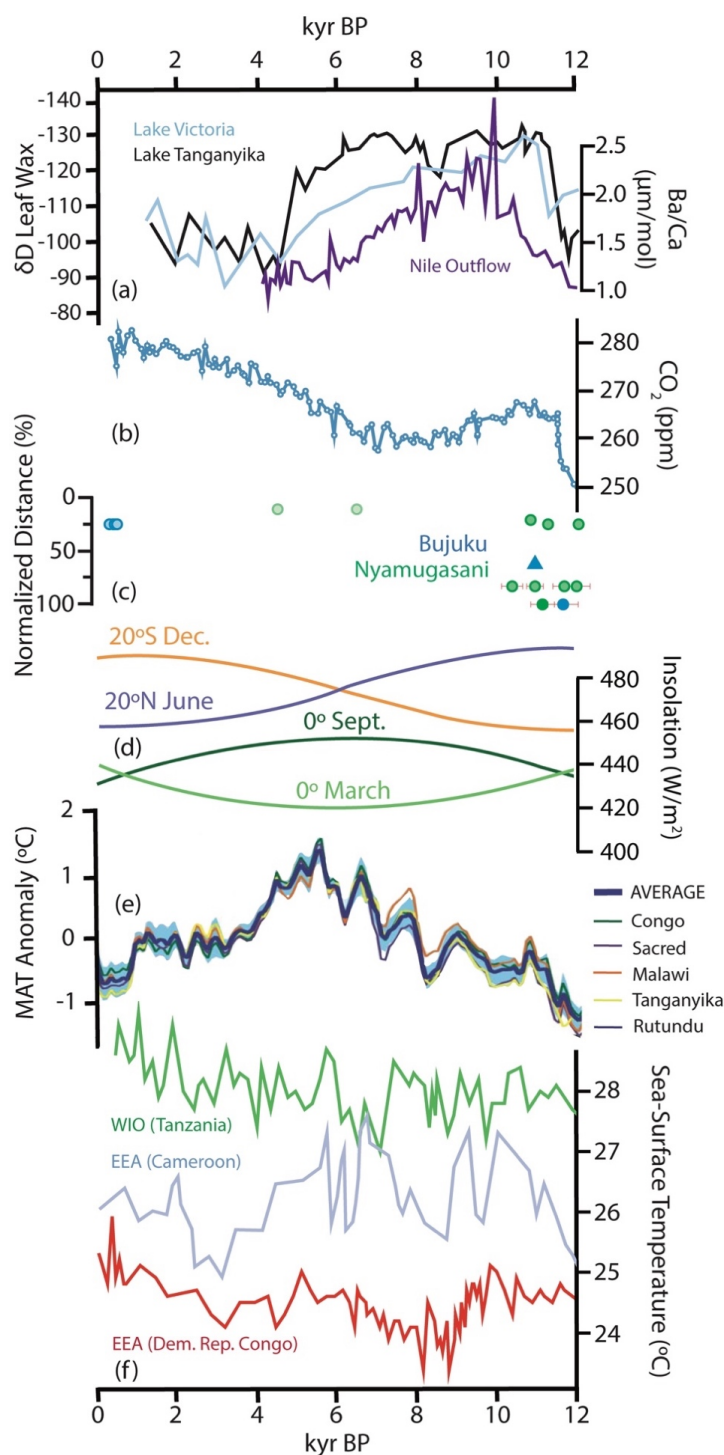


Figure 6. East African climate during the Holocene. (a) Precipitation (δD leaf wax) records from Lakes Victoria (light blue) and Tanganyika (black) and East Asian monsoon intensity (purple; Ba/Ca) from the Nile Delta (Tierney et al., 2008; Berke et al., 2012; Weldeab et al., 2014); (b) Atmospheric CO_2 (Monnin et al., 2001); (c) Normalized glacier distance down valley in the Nyamugasani (green) and Bujuku (blue) valleys in the Rwenzori Mountains as in Figure 5.; (d) Tropical Holocene insolation at $20^\circ N$ (June; blue), $20^\circ S$ (Dec.; orange), and 0° (Sept. (dark green) and March (light green) (Berger and Loutre, 1991); (e) Holocene terrestrial temperatures reconstructed from organic lacustrine sediments, bootstrapped and plotted as anomaly using the mean value over the last 2 ka (Ivory et al., 2017); (f) Sea-surface temperature records from the equatorial Western Indian Ocean (WIO; green; Romahn et al., 2014) and the Eastern Atlantic (EEA; light blue, red; Weldeab et al., 2005).



513 **6.3 Tropical South American Glacial Fluctuations and Implications for Holocene Climate**

514 Reconstructions of Holocene glacial fluctuations in South America show broad
 515 similarities in the timing and magnitude of tropical Andean glacial extent change with records of
 516 glacial extent from tropical Africa. Glaciers in the northern and southern tropical Andes retreated
 517 during the Early Holocene and remained near or within their Late Holocene extents throughout
 518 much of the Holocene Epoch (e.g., Jomelli et al., 2014; Stansell et al., 2017). ^{10}Be dating of Late
 519 Holocene moraines documents glacial advances in the South American tropics after ~ 2 -1 ka
 520 (Solomina et al., 2015), and many glaciers only reached their Late Holocene maximum extents
 521 within the last ~ 700 -500 years (Licciardi et al., 2009; Jomelli et al., 2011; Jomelli et al., 2014;
 522 Stansell et al., 2015; 2017). Sediment-flux analyses and radiocarbon dating of glacially
 523 influenced lake sediments, however, indicate that glaciers were more erosive, and perhaps more
 524 extensive, after ~ 5 cal kyr BP relative to earlier Holocene time (e.g., Rodbell et al., 2008). Lake
 525 sediment records from sites in the Eastern Cordillera and Cordillera Blanca of Peru suggest that
 526 glaciers in these regions advanced and retreated multiple times during the Holocene, with more
 527 advanced ice positions taking hold after ~ 4 -2 cal kyr BP (Rodbell et al., 2008; Stansell et al.,
 528 2015; 2017). ^{10}Be dating and geomorphic mapping of moraines from these sites also suggest that
 529 glaciers generally remained inboard of their Late Holocene maxima until at least ~ 1 ka (Stansell
 530 et al., 2015; 2017). Altogether these data suggest that, after a period of Early Holocene retreat,
 531 glacial margins in the South American tropics were more dynamic after ~ 5 ka relative to the
 532 Early Holocene but did not achieve their maximum extents until after ~ 1 ka.

533 The broad similarity of Holocene glacial fluctuations in tropical East Africa and South
 534 America suggests that tropical glaciers responded to a common, pan-tropical forcing mechanism
 535 during the Holocene. Based upon prior observational and modeling work assessing controls on



536 glacial mass balance across the South American Cordillera (Sagredo and Lowell, 2012; Sagredo
537 et al., 2014), we suggest that temperature was the primary control on glacial extents across the
538 low latitudes during the Holocene. This hypothesis requires that Holocene temperatures were
539 similar across the tropics, and that whatever mechanism or mechanisms affected temperatures in
540 one region had similar impact elsewhere. As in East Africa, radiative forcing from atmospheric
541 CO₂ and mean-annual or seasonal equatorial insolation cannot easily explain the pattern of
542 glacial fluctuations in the South American tropics. This highlights an avenue for future research
543 through both ground-based geologic investigation as well as through climate and mass-balance
544 modeling. Determining the mechanisms that influence temperatures in the low latitudes is crucial
545 for understanding better the context for modern warming and the sensitivity of tropical glaciers
546 to future climate change.

547

548 **7 Conclusions**

549 Twelve new ¹⁰Be ages of glacial features in the Rwenzori Mountains indicate that glaciers
550 retreated rapidly during the Early Holocene and remained near or within their Late Holocene
551 extents through much of the Holocene Epoch. These results are broadly similar to records of past
552 glacial fluctuations elsewhere in tropical East Africa. Based on a comparison of tropical East
553 African glacial fluctuations with regional climate records, we suggest that temperature acted as
554 the primary control on glacial fluctuations throughout the Holocene.

555 Glacial chronologies from tropical Africa and South America indicate that Early
556 Holocene glacial recession was followed by a period of generally restricted ice extents until at
557 least ~ 1 ka. The coherence of tropical African and South American glacial fluctuations suggests
558 that glaciers across the low latitudes responded to a common forcing during the Holocene, which



559 we suggest was most likely temperature. However the ultimate driver of Holocene temperatures,
560 and thus glacial extent, remains enigmatic. Understanding the controls on low-latitude
561 temperature is crucial for assessing and contextualizing modern climate variability and for
562 determining the sensitivity of tropical glaciers to changing climate conditions. Although more
563 work is needed to assess the sensitivity of low-latitude temperature to discrete forcing
564 mechanisms, the results presented here highlight the utility of glacial records in assessing past
565 terrestrial temperature change in tropical regions.

566

567

568

569

570

571

572

573

574

575

576

577

578

579

580

581



582 **Data Availability**

583 All analytical information and metadata associated with newly reported cosmogenic nuclide
584 measurements are included within the manuscript tables (Tables 1-3). All reported cosmogenic
585 nuclide ages are as calculated using the ICE-D calibration database (calibration.ice-d.org) and
586 version 3 of the online exposure-age calculator as described by Balco et al., 2008 and
587 subsequently updated (hess.ess.washington.edu).

588

589 **Author Contribution**

590 MK, JR, and AD designed the project. BN coordinated the project in Uganda. MJ, AD, JR, and
591 MK collected samples. MJ and JH processed samples for ^{10}Be dating and SRHZ measured
592 beryllium ratios. MJ, MK, AD, and JR analyzed results. MJ wrote the paper with contributions
593 from all authors.

594

595 **Competing Interests**

596 The authors declare that they have no competing interests.

597

598 **Acknowledgements**

599 We thank the Uganda Wildlife Authority and the Uganda National Council on Science and
600 Technology for their support of and assistance with this project. We also thank Rwenzori
601 Mountaineering Services and Rwenzori Trekking Services for their logistical support while in
602 the field. Laura Hutchinson and David Cavagnaro helped process samples. This project was
603 supported by the National Science Foundation (EAR-1702293; GSS-1558358), Comer Science
604 and Education Foundation (CP103), Comer Global Climate Change Foundation (GCCF13), and



605 Sigma Xi (G20141015664263). Satellite imagery was granted by the DigitalGlobe Foundation
606 (0054508271). This is LLNL-JRNL-807478.

607

608

609

610

611

612

613

614

615

616

617

618

619

620

621

622

623

624

625

626

627



628 References

- 629 Abruzzi, L.: The snows of the Nile. *Geographic Journal*, pp. 121-147. 1907.
 630
 631 Balco, G., Stone, J.O., Lifton, N.A. and Dunai, T.J.: A complete and easily accessible
 632 means of calculating surface exposure ages or erosion rates from ^{10}Be and ^{26}Al
 633 measurements. *Quaternary Geochronology* 3, 174-195. 2008.
 634
 635 Berger, A. and Loutre, M.F.: Insolation values for the climate of the last 10 million
 636 years. *Quaternary Science Reviews* 10, 297-317. 1991.
 637
 638 Bergström, E.: British Ruwenzori Expedition, 1952 Glaciological Observations—Preliminary
 639 Report. *Journal of Glaciology* 2, 469-476. 1955.
 640
 641 Berke, M.A., Johnson, T.C., Werne, J.P., Grice, K., Schouten, S. and Damsté, J.S.S.: Molecular
 642 records of climate variability and vegetation response since the Late Pleistocene in the Lake
 643 Victoria basin, East Africa. *Quaternary Science Reviews* 55, 9-74. 2012.
 644
 645 Bradley, R.S., Vuille, M., Diaz, H.F. and Vergara, W.: Threats to water supplies in the tropical
 646 Andes. *Science* 312, 1755-1756. 2006.
 647
 648 Beuning, K.R.M. and Russell, J.M. Vegetation and sedimentation in the Lake Edward basin,
 649 Uganda-Congo during the late Pleistocene and early Holocene.: *Journal of Paleolimnology* 32,
 650 1-18. 2004.
 651
 652 Cavagnaro, D.B.: Cosmogenic ^{10}Be exposure dating of a post-glacial landslide in the Rwenzori
 653 Mountains, Uganda. Undergraduate thesis, Dartmouth College, Hanover NH, United States. 36
 654 pp. 2017.
 655
 656 Chevallier, P., Pouyaud, B., Suarez, W. and Condom, T.: Climate change threats to environment
 657 in the tropical Andes: glaciers and water resources. *Regional Environmental Change* 11, 179-
 658 187. 2011.
 659
 660 Doughty, A.M., Kelly, M.A., Russell, J.M., Jackson, M.S., Anderson, B.M., Chipman, J.,
 661 Nakileza, B., and Dee, S.G.: The dynamics of Equilibrium Line Altitudes in over the past 31,000
 662 years in the Rwenzori Mountains, East Africa. *GSA Special Paper on Quaternary Science in*
 663 *honor of Prof. Stephen C. Porter [in press]*.
 664
 665 Dunai, T.J.: Cosmogenic Nuclides: Principles, concepts and applications in the Earth surface
 666 sciences. Cambridge University Press. 2010.
 667
 668 Foster, P.: The potential negative impacts of global climate change on tropical montane cloud
 669 forests, *Earth Science Reviews* 55, 73–106. 2001.
 670



- 671 Gabrielli, P., Hardy, D.R., Kehrwald, N., Davis, M., Cozzi, G., Turetta, C., Barbante, C. and
 672 Thompson, L.G.: Deglaciated areas of Kilimanjaro as a source of volcanic trace elements
 673 deposited on the ice cap during the late Holocene. *Quaternary Science Reviews* 93, 1-10. 2014.
- 674 Garcin, Y., Vincens, A., Williamson, D., Buchet, G., and Guiot, J.: Abrupt resumption of the
 675 African Monsoon at the Younger Dryas-Holocene climatic transition. *Quaternary Science*
 676 *Reviews* 26, 690-704. 2007.
- 677 Hamilton, A. and Perrott, A.: Date of deglaciation of Mount Elgon. *Nature* 273, 49-49. 1978.
 678
- 679 Ivory, S.J. and Russell, J.: Lowland forest collapse and early human impacts at the end of the
 680 African Humid Period at Lake Edward, equatorial East Africa. *Quaternary Research* 89, 7-20.
 681 2017.
 682
- 683 Jackson, M.S., Kelly, M.A., Russell, J.M., Doughty, A.M., Howley, J.A., Cavagnaro, D.B.,
 684 Zimmerman, S.R.H., and Nakileza, B.: Glacial fluctuations in tropical Africa during the last
 685 glacial termination and implications for tropical climate following the Last Glacial Maximum.
 686 *Quaternary Science Reviews* [in review].
 687
- 688 Jackson, M.S., Kelly, M.A., Russell, J.M., Doughty, A.M., Howley, J.A., Chipman, J.W.,
 689 Cavagnaro, D., Nakileza, B. and Zimmerman, S.R.: High-latitude warming initiated the onset of
 690 the last deglaciation in the tropics. *Science Advances*, 5(12), eaaw2610. 2019.
- 691 Johansson, L., and Holmgren, K.: Dating of a moraine on Mount Kenya. *Geografiska Annaler*
 692 *Series A Physical Geography* 67, 123-128. 1985.
- 693 Jomelli, V., Khodri, M., Favier, V., Brunstein, D., Ledru, M.-P., Wagnon, P., Blard, P.-H.,
 694 Sicart, J.-E., Braucher, R., Grancher, D., Bourlès, D.L., Braconnot, P., and Vuille, M.: Irregular
 695 tropical glacier retreat over the Holocene epoch driven by progressive warming. *Nature* 474,
 696 196–199. 2011.
- 697 Jomelli, V., Favier, V., Vuille, M., Braucher, R., Martin, L., Blard, P.-H., Colose, C., Brunstein,
 698 D., He, F., Khodri, M., Bourlès, D.L., Leanni, L., Rinterknecht, V., Grancher, D., Francou, B.,
 699 Ceballos, J.L., Fonseca, H., Liu, Z., and Otto-Bleisner, L.: A major advance of tropical Andean
 700 glaciers during the Antarctic cold reversal. *Nature* 513, 224-228. 2014.
- 701 Karlén, W., Fastook, J.L., and Holmgren, K.: Glacier Fluctuations on Mount Kenya since-6000
 702 Cal. Years BP: Implications for Holocene Climatic Change in Africa. *Ambio* 28, 409-418. 1999.
- 703 Kaser, G., Mölg, T., Cullen, N.J., Hardy, D.R., and Winkler, M.: Is the decline of ice on
 704 Kilimanjaro unprecedented in the Holocene? *The Holocene* 20, 1079–1091. 2010.
- 705 Kaser, G. and Osmatson, H. Tropical Glaciers. Cambridge, Cambridge University Press, 207 pp.
 706 2002.



- 707 Kelly, M.A.: The Late Würmian Age in the Western Swiss Alps: Last Glacial Maximum (LGM)
 708 Ice-surface Reconstruction and ^{10}Be Dating of Late-glacial Features. PhD thesis, University of
 709 Bern, Switzerland. 2003.
- 710 Kelly, M.A., Russell, J.M., Baber, M.B., Howley, J.A., Loomis, S.E., Zimmerman, S., Nakileza,
 711 R., and Lukaye, J. Expanded glaciers during a dry and cold Last Glacial Maximum in equatorial
 712 East Africa. *Geology* 42, 519-522. 2014.
- 713 Kelly, M.A., Lowell, T.V., Applegate, P.J., Phillips, F.M., Schaefer, J.M., Smith, C.A., Kim, H.,
 714 Leonard, K.C., Hudson, A.M.: A locally calibrated, late glacial ^{10}Be production rate from a low-
 715 latitude, high-altitude site in the Peruvian Andes. *Quaternary Geochronology* 26, 1–16. 2015.
- 716 Lal, D.: Cosmic ray labeling of erosion surfaces: in situ nuclide production rates and erosion
 717 models. *Earth and Planetary Science Letters* 104, 424–439. 1991.
- 718 Licciardi, J.M., Schaefer, J.M., Taggart, J.R., and Lund, D.C.: Holocene Glacier Fluctuations in
 719 the Peruvian Andes Indicate Northern Climate Linkages. *Science* 325, 1677–1679. 2009.
- 720 Lifton, N.: Implications of two Holocene time-dependent geomagnetic models for cosmogenic
 721 nuclide production rate scaling. *Earth and Planetary Science Letters* 433, 257–268. 2016.
- 722 Livingstone, D.A.: Postglacial vegetation of the Ruwenzori Mountains in equatorial Africa.
 723 *Ecological Monographs* 37, 25-52. 1967.
- 724 Loomis, S.E., Russell, J.M., Ladd, B., Street-Perrott, F. A., and Sinninghe Damsté, J.S.:
 725 Calibration and application of the branched GDGT temperature proxy on East African lake
 726 sediments. *Earth and Planetary Science Letters* 375-378, 277-288. 2012.
- 727 Loomis, S.E., Russell, J.M., Verschuren, D., Morrill, C., De Cort, G., Damsté, J.S.S., Olago, D.,
 728 Eggermont, H., Street-Perrott, F.A., and Kelly, M.A.: The tropical lapse rate steepened during
 729 the Last Glacial Maximum. *Science Advances* 3, e1600815. 2017.
- 730 Mahaney, W.C., e.d. Quaternary and Environmental Research on East African Mountains. CRC
 731 Press. 1989.
- 732 McConnell, R.B.: Outline of the geology of the Ruwenzori Mountains, a preliminary account of
 733 the results of the British Ruwenzori expedition, 1951-1952. *Overseas Geology and Mineral*
 734 *Resources* 7, 245-268. 1959.
- 735 McGlynn, G., Mackay, A.W., Rose, N.L., Taylor, R.G., Leng, M.J. and Engstrom, D.R.:
 736 Palaeolimnological evidence of environmental change over the last 400 years in the Rwenzori
 737 Mountains of Uganda. *Hydrobiologia* 648, 109-122. 2010.
- 738 Meader, M., 1937. *From the University of Wisconsin Milwaukee AGSL Photo Library*
 739 [<https://collections.lib.uwm.edu/digital/collection/agsafrica/id/358/rec/102>]



- 740 Mölg, T., Hardy, D.R. and Kaser, G.: Solar-radiation-maintained glacier recession on
 741 Kilimanjaro drawn from combined ice-radiation geometry modeling. *Journal of Geophysical*
 742 *Research: Atmospheres* 108 (D23). 2003a
- 743 Mölg, T., Georges, C., and Kaser, G.: The contribution of increased incoming shortwave
 744 radiation to the retreat of the Rwenzori glaciers, East Africa, during the 20th century.
 745 *International Journal of Climatology* 23, 291-303. 2003b.
- 746 Monnin, E., Indermühle, A., Dällenbach, A., Flückiger, J., Stauffer, B., Stocker, T.F., Raynaud,
 747 D., and Barnola, J.M.: Atmospheric CO₂ concentrations over the last glacial termination. *Science*
 748 291, 112-114. 2001.
- 749 Nishiizumi, K., Imamura, M., Caffee, M.W., Southon, J.R., Finkel, R.C., and McAninch, J.:
 750 Absolute calibration of Be-10 AMS standards. *Nuclear Instruments and Methods in Physics*
 751 *Research Section B* 285B, 403-413. 2007.
- 752 Noell, A.C., Abbey, W.J., Anderson, R.C., and Ponce, A.: Radiocarbon dating of glacial dust
 753 layers and soils at Kilimanjaro's Northern Ice Field. *The Holocene* 24, 1398-1405. 2014.
- 754 Osmaston, H.: The past and present climate and vegetation of the Ruwenzori and its
 755 neighborhood. Ph.D. Thesis, Oxford University. 140 pp. 1965.
- 756 Osmaston, H.A. and Pasteur, D.: Guide to the Ruwenzori. Alden Press, Oxford, pp. 200. 1972.
- 757 Osmaston, H.: Glaciers, glaciations, and equilibrium line altitudes on the Rwenzori. In Mahaney,
 758 W.C. (Ed.) Quaternary and environmental research on East African mountains. Rotterdam,
 759 Balkema, 31-104. 1989.
- 760 Perrott, R.A.: A high altitude pollen diagram from Mount Kenya: Its implications for the history
 761 of glaciation. In Coetzee J.A. and van Zinderen Bakker, E.M. (eds). *Paleoecology of Africa* 14,
 762 77-83. 1982.
- 763 Plug, L.J., Gosse, J.C., McIntosh, J.J., and Bigley, R.: Attenuation of cosmic ray flux in
 764 temperate forest. *Journal of Geophysical Research* 112, F02022. 2007.
- 765 Ring, U.: Extreme uplift of the Rwenzori Mountains in the East African Rift, Uganda: Structural
 766 framework and possible role of glaciations. *Tectonics* 27. 2008.
- 767 Rodbell, D.T., Seltzer, G.O., Mark, B.G., Smith, J.A., and Abbott, M.B.: Clastic sediment flux to
 768 tropical Andean lakes: records of glaciation and soil erosion. *Quaternary Science Reviews* 27,
 769 1612-1626. 2008.
- 770 Romahn, N., Baumann, K.-H., and Pätzold, J.: Thermocline fluctuations in the western tropical
 771 Indian Ocean during the past 35 ka. *Journal of Quaternary Science* 30, 201-210. 2015.
 772



- 773 Russell, J.M., Johnson, T.C., Kelts, K.R., Laerdal, T., and Talbot, M.R.: An 11,000 year
 774 lithostratigraphic and paleohydrologic record from equatorial Africa: Lake Edward, Uganda-
 775 Congo. *Palaeogeography, Palaeoclimatology, Palaeoecology* 193, 25–49. 2003a.
 776
- 777 Russell, J.M., Johnson, T.C., and Talbot, M.R.: A 725 yr cycle in the climate of central Africa
 778 during the Late Holocene. *Geology* 31, 677–680. 2003b.
- 779 Russell, J.M. and Johnson, T.C.: The water balance and stable isotope hydrology of Lake
 780 Edward, Uganda-Congo. *Journal of Great Lakes Research* 32, 77–90. 2006.
- 781 Russell, J.M., Eggermont, H.E., Taylor, R., and Verschuren, D.: Paleolimnological records of
 782 recent glacier recession in the Rwenzori Mountains, Uganda-D.R. Congo. *Journal of*
 783 *Paleolimnology* 41, 253–271. 2009.
- 784 Sagredo, E.A. and Lowell, T.V.: Climatology of Andean glaciers: A framework to understand
 785 glacier response to climate change. *Global and Planetary Change* 86–87, 101–109. 2012.
- 786 Sagredo, E.A., Rupper, S., and Lowell, T.V.: Sensitivities of the equilibrium line altitude to
 787 temperature and precipitation changes along the Andes. *Quaternary Research* 81, 355–366.
 788 2014.
- 789 Schaefer, J.M., Kaplan, M., Putnam, A., and Schlüchter, C.: Southern mid-latitude terminations
 790 of MIS-4, the Last Glacial Maximum and the Late Glacial period in the New Zealand moraine
 791 record. *Geochimica et cosmochimica acta* 73, 29–29. 2009.
- 792 Shanahan, T. and Zreda, M.: Chronology of Quaternary glaciations in East Africa. *Earth and*
 793 *Planetary Science Letters* 177, 23–42. 2000.
- 794 Singarayer, J.S. and Burrough, S.L.: Interhemispheric dynamics of the African rainbelt during
 795 the late Quaternary. *Quaternary Science Reviews* 124, 48–67. 2015.
- 796 Solomina, O.N., Bradley, R.S., Hodgson, D.A., Ivy-Ochs, S., Jomelli, V., Mackintosh, A.N.,
 797 Nesje, A., Owen, L.A., Wanner, H., Wiles, G.C., and Young, N.E.: Holocene glacier
 798 fluctuations. *Quaternary Science Reviews* 111, 9–34. 2015.
- 799 Stansell, N.D., Rodbell, D.T., Licciardi, J.M., Sedlak, C.M., Schweinsberg, A.D., Huss, E.G.,
 800 Delgado, G.M., Zimmerman, S.H., and Finkel, R.C.: Late Glacial and Holocene glacier
 801 fluctuations at Nevado Huaguruncho in the Eastern Cordillera of the Peruvian Andes. *Geology*
 802 G36735.1–4. 2015.
- 803 Stansell, N.D., Licciardi, J.M., Rodbell, D.T., and Mark, B.G.: Tropical ocean- atmospheric
 804 forcing of Late Glacial and Holocene glacier fluctuations in the Cordillera Blanca, Peru.
 805 *Geophysical Research Letters* 44, 4176–4185. 2017.
- 806 Stocker, T.F., Qin, D., Plattner, G.K., Tignor, M., Allen, S.K., Boschung, J., Nauels, A., Xia, Y.,
 807 Bex, V., and Midgley, P.M.: IPCC, 2013: Climate Change 2013: The Physical Science Basis.



- 808 Contribution of Working Group I to the Fifth Assessment Report of the Intergovernmental Panel
 809 on Climate Change, 1535 pp. 2013.
- 810 Stone, J.O.: Air pressure and cosmogenic isotope production. *Journal of Geophysical Research*
 811 105, 23753-23759. 2000.
- 812 Taylor, R.G., Mileham, L., Tindimugaya, C., Majugu, A., Muwanga, A., and Nakileza, B.:
 813 Recent glacial recession in the Ruwenzori Mountains of East Africa due to rising air
 814 temperature. *Geophysical Research Letters* 33, L10402. 2006.
- 815 Thompson, L.G., Mosley-Thompson, E., Davis, M.E., Henderson, K.A., Brecher, H.H.,
 816 Zagorodnov, V.S., Mashiotto, T.A., Lin, P.N., Mikhalevko, V.N., Hardy, D.R., and Beer, J.:
 817 Kilimanjaro ice core records: Evidence of Holocene climate change in tropical Africa. *Science*
 818 298, 589–593. 2002.
- 819 Thompson, L.G., Mosley-Thompson, E., Davis, M., and Mountain, K.: A paleoclimatic
 820 perspective on the 21st-century glacier loss on Kilimanjaro, Tanzania. *Annals of Glaciology* 52,
 821 60-68. 2011.
- 822 Tiercelin, J.J., Gibert, E., Umer, M., Bonnefille, R., Disnar, J.R., Lézine, A.M., Hureau-
 823 Mazaudier, D., Travi, Y., Keravis, D., and Lamb, H.F.: High-resolution sedimentary record of
 824 the last deglaciation from a high-altitude lake in Ethiopia. *Quaternary Science Reviews* 27, 449–
 825 467. 2008.
- 826 Tierney, J.E., Russell, J.M., Huang, Y., and Damsté, J.: Northern hemisphere controls on tropical
 827 southeast African climate during the past 60,000 years. *Science* 322, 252-255. 2008.
- 828 Vuille, M., Francou, B., Wagnon, P., Juen, I., Kaser, G., Mark, B.G., and Bradley, R.S.: Climate
 829 change and tropical Andean glaciers: Past, present and future. *Earth-Science Reviews* 89, 79-96.
 830 2008.
- 831 Walker, M.J., Berkelhammer, M., Björck, S., Cwynar, L.C., Fisher, D.A., Long, A.J., Lowe, J.J.,
 832 Newnham, R.M., Rasmussen, S.O. and Weiss, H.: Formal subdivision of the Holocene
 833 Series/Epoch: a Discussion Paper by a Working Group of INTIMATE (Integration of ice-core,
 834 marine and terrestrial records) and the Subcommittee on Quaternary Stratigraphy (International
 835 Commission on Stratigraphy). *Journal of Quaternary Science* 27, 649-659. 2012.
- 836 Weijers, J.W.H., Schefuss, E., Schouten, S., and Damste, J.S.S.: Coupled Thermal and
 837 Hydrological Evolution of Tropical Africa over the Last Deglaciation. *Science* 315, 1701–1704.
 838 2007.
- 839 Weldeab, S., Schneider, R.R., Kölling, M., and Wefer, G.: Holocene African droughts relate to
 840 eastern equatorial Atlantic cooling. *Geology* 33, 981-984. 2005.
- 841 Weldeab, S., Menke, V., and Schmiedl, G.: The pace of East African monsoon evolution during
 842 the Holocene. *Geophysical Research Letters* 41, 1724-1732. 2014.



- 843 Whittow, J.B., Shepherd, A., and Goldthorpe, J.E.: Observations on the glaciers of the
844 Ruwenzori. *Journal of Glaciology* 4, 581-616. 1963.
- 845 Woltering, M., Johnson, T.C., Werne, J.P., Schouten, S., and Damsté, J.S.S.: Late Pleistocene
846 temperature history of Southeast Africa: a TEX86 temperature record from Lake Malawi.
847 *Palaeogeography, Palaeoclimatology, Palaeoecology* 303, 93-102. 2011.